RESEARCH ARTICLE

Hydrography-Driven Coarsening of Grid Digital Elevation Models

Giovanni Moretti[1] (ID) and Stefano Orlandini[1] (ID)

[1]Dipartimento di Ingegneria Enzo Ferrari, Università degli Studi di Modena e Reggio Emilia, Modena, Italy

Key Points:
- A new strategy for coarsening high-resolution grid digital elevation models is developed to retain observed valley and channel profiles
- This hydrography-driven coarsening strategy yields valleys and channels that compare favorably with those observed
- The hydrography-driven coarsening drastically reduces the impact of depression-filling in the obtained coarse digital elevation models

Correspondence to:
S. Orlandini,
stefano.orlandini@unimore.it

Abstract A new grid coarsening strategy, denoted as hydrography-driven coarsening, is developed in the present study. The hydrography-driven coarsening is designed to retain the essential hydrographic features of valleys and channels observed in high-resolution digital elevation models: (1) depressions are filled in the considered high-resolution digital elevation model, (2) the obtained topographic data are used to extract a reference grid network composed of all surface flow paths, (3) the Horton order is assigned to each link of the reference grid network, and (4) within each coarse grid cell, the elevation of the point lying along the highest-order path of the reference grid network and displaying the minimum distance to the cell center is assigned to this coarse grid cell center. The capabilities of the hydrography-driven coarsening to provide consistent surface flow paths with respect to those observed in high-resolution digital elevation models are evaluated over a synthetic valley and two real drainage basins located in the Italian Alps and in the Italian Apennines. The hydrography-driven coarsening is found to yield significantly more accurate valley and channel profiles than existing coarsening strategies. In absolute terms, the obtained valleys and channels compare favorably with those observed. In addition, the proposed coarsening strategy is found to reduce drastically the impact of depression-filling in the obtained coarse digital elevation models. The hydrography-driven coarsening strategy is therefore advocated for all those cases in which the relief of the extracted drainage network is an important hydrographic feature.

Plain Language Summary High-resolution digital elevation models (grid cell size of 1 m or less) generated from light detection and ranging (lidar) surveys are making detailed topographic descriptions of drainage basins increasingly available. On the other hand, grid coarsening is often necessary to meet computational constrains in detailed, large-scale, and/or long-term hydrologic simulations. While nearest neighbor coarsening remains the standard strategy, more complex coarsening strategies with special focus on drainage basin hydrology have recently been proposed. However, existing coarsening strategies may not capture important hydrographic features observed in high-resolution topographic data. Existing coarsening strategies may cause significant alterations of land surface topography, especially when depression-filling procedures are applied to coarsened digital elevation models. It is, therefore, relevant to seek grid coarsening strategies that can better retain the hydrographic features observed in high-resolution digital elevation models, and that can have beneficial implications on the description of surface flow propagation, hyporheic fluxes, and hydrologic interactions between hill slope and channel networks. A hydrography-driven coarsening strategy is developed and tested in the present study. This strategy is found to significantly improve the capabilities of existing coarsening strategies to yield accurate descriptions of valleys and channels in coarse digital elevation models.

1. Introduction

Digital elevation models are used to describe land surface topography and related attributes (e.g., Bonetti et al., 2018; Gallant & Hutchinson, 2011; Wilson & Gallant, 2000). Gridded (regular network) or triangulated irregular network digital elevation models are commonly used to define the computational meshes of distributed hydrologic models (e.g., Ivanov et al., 2004; Orlandini & Rosso, 1998). In addition, it has been shown that flow nets can be automatically constructed from contour elevation data (Moretti & Orlandini, 2008). High-resolution (1 m or less) grid digital elevation models based on light detection and ranging (lidar) surveys are making detailed topographic descriptions of hill slopes and drainage basins increasingly available

(e.g., Orlandini et al., 2012; Tarolli, 2014). However, grid (or network) coarsening is often necessary to meet computational constrains in detailed, large-scale, and/or long-term hydrologic simulations (e.g., Camporese et al., 2010; Kollet & Maxwell, 2006; Wilby et al., 2000). The nearest neighbor coarsening strategy is commonly used in drainage basin hydrology to resample digital elevation models (e.g., De Bartolo et al., 2016; Le Coz et al., 2009; Orlandini & Moretti, 2009). However, especially when high-resolution data are coarsened to a regular grid, this coarsening strategy may not capture relevant hydrographic features displayed by high-resolution digital elevation models within the coarse grid cells. From a hydrologic point of view, it is especially important to preserve the profiles of valleys and channels within the drainage basin.

One of the most exciting opportunities offered by grid digital elevation models is to enabling the automatic extraction of drainage and channel networks (e.g., Montgomery & Foufoula-Georgiou, 1993; Orlandini et al., 2011). The channel network is the pattern of tributaries and master streams in a drainage basin as delineated on a planimetric map (Leopold et al., 1964, p. 131). Channel network relief is also important in hydrology and geomorphology (Bras, 1990, p. 582). Commonly used methods for the extraction of channel networks in grid digital elevation models imply generally three essential steps: (1) removal of pits or depressions, (2) determination of surface slope directions and related surface flow paths forming the grid network, and (3) identification of the channel network as the portion of the grid network extending downstream the channel heads (e.g., Orlandini et al., 2011). In the first step, all the cells of the raw digital elevation model with except for the outlet cell are processed in such a way to remove pits, that are cells having no neighbors at a lower elevation (e.g., Barnes et al., 2014; Grimaldi et al., 2007; Hutchinson, 1989; Martz & Garbrecht, 1992). This facilitates the second and third steps, in which surface flow paths are obtained by connecting grid cell centers along predetermined slope directions and the channel network is identified by using threshold quantities for channel initiation computed over the extracted grid network (e.g., Gallant & Wilson, 2000; Orlandini et al., 2003, 2011, 2014). However, especially when standard nearest neighbor coarsening is used to describe complex terrains, depression-filling procedures may cause local errors due to inappropriate coarsening to propagate to upstream drainage areas, with significant alterations of the channel network relief and potential implications on the description of surface flow propagation, hyporheic fluxes, and hydrologic interactions between hill slope and channel networks (e.g., Hester & Doyle, 2008; McGuire & McDonnell, 2010; Orlandini & Rosso, 1998).

There is therefore a need to make a better use of high-resolution topographic data based on lidar surveys in distributed hydrologic models so that relevant hydrographic features of valleys and channels observed in high-resolution topographic data are retained in coarse digital elevation models. Specific methods have recently been developed to extract channels directly from high-resolution digital elevation models, but the direct use of these extracted channels in distributed hydrologic models remains a challenge (e.g., Passalacqua et al., 2010a, 2010b, 2015). Methods for the determination of slope directions in coarse-resolution (1–4 km) distributed hydrologic models have been developed by analyzing higher-resolution digital elevation models within each coarse grid cell (e.g., O'Donnell et al., 1999; Reed, 2003; Wang et al., 2000). Other possible strategies for preserving the channel network structure in coarse digital elevation models have been experimented by seeking the optimal degree of smoothing or the most effective constrains in high-resolution topographic data (e.g., Chen et al., 2012; Le Coz et al., 2009; Zhou & Chen, 2011). In Chen et al. (2012), Zhou and Chen's (2011) compound method was shown to outperform the ANUDEM coarsening strategy developed by Hutchinson (1989) and the stream burning algorithm developed by Saunders (2000) when digital elevation models having a resolution greater than or equal to 3 m are used as input raster. However, the capability of Zhou and Chen's (2011) compound method to convey hydrographic features observed in high-resolution (1 m or less) topographic data to significantly coarser grid digital elevation models has not been tested so far.

In the present study, a different modeling philosophy is adopted by identifying and directly using the hydrographically most significant elevations observed in high-resolution topographic data and in the related network of surface flow paths. The resulting hydrography-driven coarsening strategy is designed to convey the essential features of valleys and channels observed in high-resolution topographic data directly to coarse grid digital elevation models so that the structure of the drainage network is preserved and the impact of depression-filling is minimized. No filtering or interpolation of high-resolution topographic data is applied, and results are evaluated against hydrographic features observed in high-resolution topographic data. Digital elevation models and extracted drainage networks obtained from the proposed coarsening
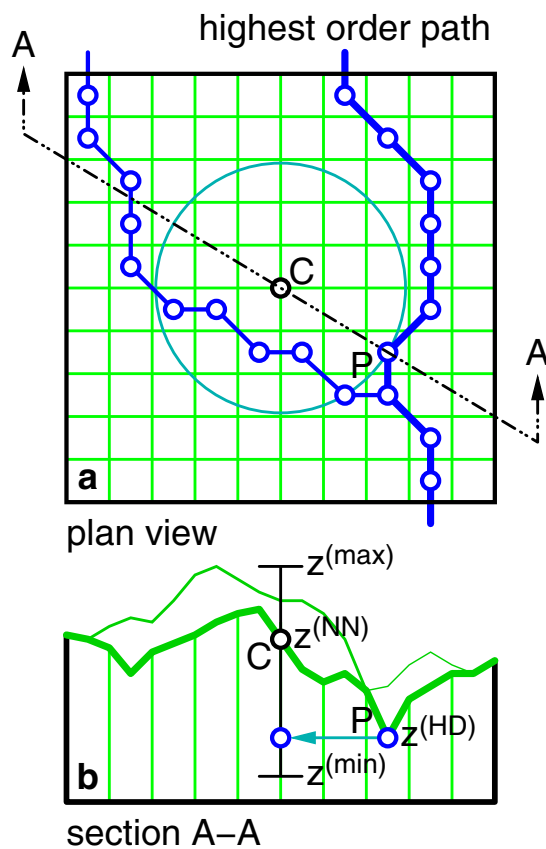
Figure 1. Sketch of the hydrography-driven (HD) coarsening. When coarsening a high-resolution grid (green cells in Figure 1a) to a coarse-resolution grid (back cell in Figure 1a), the nearest neighbor (NN) elevation to the coarse grid cell center C ($z^{(NN)}$ in Figure 1b), or some kind of average elevation lying between the minimum and maximum terrain elevations observed within the coarse cell ($z^{(min)}$ and $z^{(max)}$, respectively, in Figure 1b), is commonly assigned to the coarse grid cell center C. The HD coarsening assigns to the coarse grid cell center C the elevation of the closest point P lying along the highest Horton order surface flow path observed in high-resolution topographic data within the coarse grid cell ($z^{(HD)}$ in Figure 1b).

strategy, from standard nearest neighbor coarsening, and from Zhou and Chen's (2011) compound method are evaluated by using high-resolution digital elevation models and related drainage networks as a reference. Drainage basins located in the Italian Apennines and in the Italian Alps are considered to test the proposed coarsening strategy under different geomorphological settings.

2. Methods

The attention is focused in the present study on coarsening methods that can be used in drainage basin hydrology and geomorphology to transform a fine-resolution grid digital elevation model into a coarse-resolution grid digital elevation model. A new hydrography-driven coarsening strategy is developed to improve the ability of resampling to retain the hydrographic features of drainage networks observed in high-resolution digital elevation models. The standard nearest neighbor coarsening strategy, the compound method proposed by Zhou and Chen (2011), and the new hydrography-driven coarsening strategy are described below. The considered coarsening strategies are used in combination with depression-filling, slope direction, and channel initiation methods needed to extract a channel network from grid digital elevation models. These tasks are performed in the present study by using satisfactory methods existing in the literature, namely the priority-flood depression-filling algorithm proposed by Barnes et al. (2014), the D8-LTD slope direction algorithm proposed by Orlandini et al. (2003), and channel initiation methods investigated by Orlandini et al. (2011).

2.1. Nearest Neighbor Coarsening

The nearest neighbor (NN) coarsening is a technique for resampling raster data in which the elevation of each cell center in an output raster is calculated by using the elevation of the nearest cell center in an input raster. When more than one cell centers in the input raster are found to be equally distant to the center of the output raster cell, the average elevation over equally distant input cells is assigned to the output cell center. This is, for instance, the case of the cell center in the output raster that falls on the corner of four neighboring raster cells (e.g., cell center C in Figure 1a). The NN coarsening allows a resampled digital elevation model to preserve important geometrical properties such as symmetry of topographic structures observed in the original high-resolution digital elevation model. As sketched in Figure 1b, however, the elevations $z^{(NN)}$ observed in high-resolution topographic data in the centers of coarse grid cells may not represent the hydrographic features observed within these coarse grid cells. This limitation is especially relevant when complex topographic structures are represented by using coarse-resolution digital elevation models.

2.2. Compound Method Coarsening

The compound method (CM) coarsening developed by Zhou and Chen (2011) is selected in the present study to represent coarsening strategies proposed in the literature for improving the capabilities of the NN coarsening. A comparison between the CM and other existing coarsening strategies can be found in Chen et al. (2012). The CM coarsening is essentially composed of three phases:

1. the high-resolution digital elevation model is converted to a triangulated irregular network, namely a TIN whose surface does not deviate from the input raster by more than a specified Z-tolerance (by using the ArcGIS Raster to TIN command);
2. the obtained TIN is adapted to assigned points describing relevant hydrographic features of observed streamlines to obtain a more suitable drainage-constrained TIN; and

3. the drainage-constrained TIN resulting from phases 1 and 2 is used to determine the elevation of cell centers in the desired coarse-resolution digital elevation model (by using the ArcGIS TIN To Raster command).

When high-resolution (1 m or less) topographic data are used as input raster, phase 1 yields an accurate description of valley and channel thalwegs (i.e., the lines that connect the deepest points of bathymetric cross sections along the lengths of valleys and channels) and phase 2 becomes inessential. Under these conditions, the CM coarsening is essentially driven by phase 3 and can therefore remain susceptible to the same limitations of NN coarsening (section 2.1). This expected behavior of the CM coarsening is tested in the present study.

2.3. Hydrography-Driven Coarsening

In order to better capture the drainage basin hydrography than existing methods, a new hydrography-driven (HD) coarsening strategy is developed in the present study. In the first preparatory step of this new strategy, the reference drainage basin hydrography is extracted from the highest-resolution digital elevation model data available by using state-of-the-art methods. In this step, the priority-flood depression-filling algorithm proposed by Barnes et al. (2014) is used to remove pits and fill depressions in high-resolution digital elevation data. The loss of detail caused by depression-filling in the highest-resolution digital elevation model data is insignificant in the perspective of resampling these data to significantly lower grid resolutions. In fact, the goal of the proposed coarsening strategy is not to provide a perfect description of land surface microtopography and associated hydrography (which is clearly an impracticable task), but rather to ensure that hydrographic features observed in high-resolution digital elevation models generated from lidar surveys are retained when these data are coarsened to satisfy the computational constrains met in drainage basin hydrology. The D8-LTD slope direction algorithm proposed by Orlandini et al. (2003) is then used to extract the grid network from the obtained high-resolution topographic data. Once the reference grid network is extracted, the Horton order is assigned to each link of this network as sketched in Figure 1a.

In the second step, the hydrographic features observed in the high-resolution digital elevation model and related grid network are used to yield hydrography-driven coarse-resolution digital elevation models. Ordered surface flow paths provide a detailed description of hydrography within each cell of the output grid. The essential features of this hydrography can therefore be conveniently synthesized and retained in the resampling process. The elevation of each output cell center (e.g., point C in Figure 1) is set equal to $z^{(HD)}$, that is the elevation of the closest point lying along the highest Horton order path observed within the output cell (e.g., point P in Figure 1). The value $z^{(HD)}$ is lying between $z^{(min)}$ and $z^{(max)}$, respectively, the minimum and the maximum cell elevation of the high-resolution grid cells falling within the coarse grid cell (Figure 1b). The algorithm developed can also handle specific cases in which the edges of the coarse cell do not match the edges of high-resolution cells. These cases are handled by considering, for each coarse cell, only the high-resolution cells sharing at least 50% of their area with the coarse cell. Depression-filling is normally not needed or at most needed in a few unfortunate circumstances after HD coarsening.

3. Evaluation

NN, CM, and HD coarsening are evaluated by comparing grid and channel networks extracted in coarsened grid digital elevation models with those observed in the original high-resolution grid digital elevation model. A synthetic valley highlighting the possible impacts of coarsening methods and two real drainage basins displaying different morphological settings are considered as test cases.

3.1. Synthetic Valley

The synthetic valley (SV) is represented in Figures 2 and 3. A digital elevation model with grid cell size of 10 m is generated over a rectangular domain having size of 13 km along the x coordinate and 20 km along the y coordinate to represent a wide valley followed in a downstream direction by a deep and narrow canyon (Figure 2a). These topographic conditions can be found, for instance, in the eastern Italian Alps (e.g., Cismon, Mis, Cordevole, Maé, Piave, Cellina, and Lumiei Rivers). The SV drains from North to South, in the direction of decreasing values of y. The thalweg of the valley has x coordinate $x_t = 0$ for $10,000 \leq y \leq 20,000$ m, and
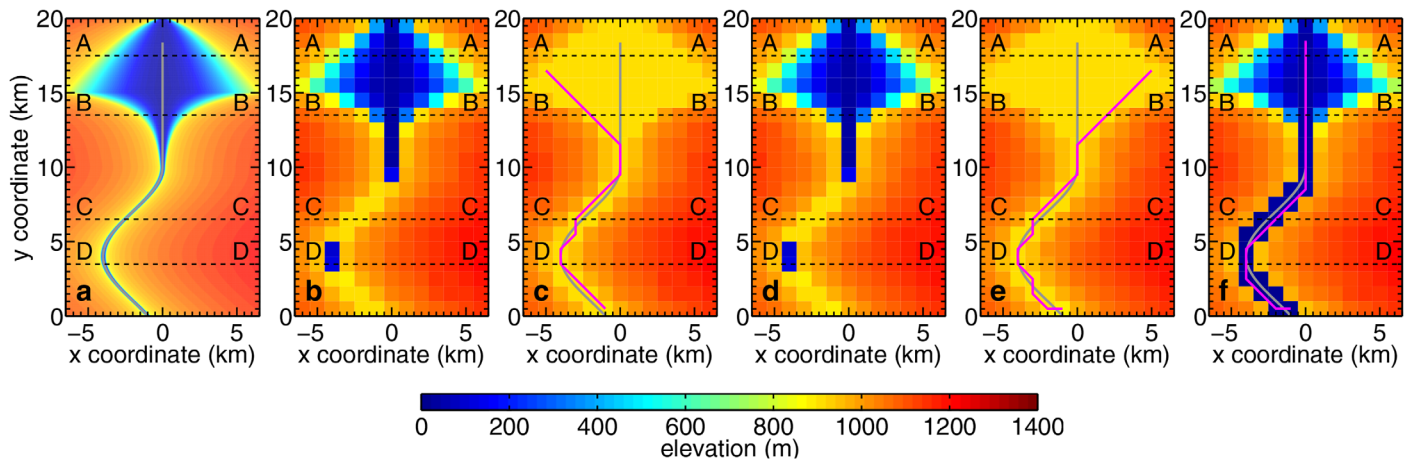
Figure 2. Digital elevation models of a synthetic valley and extracted surface flow paths. (a) 10 m grid digital elevation model displaying no depressions and extracted surface flow path (gray line) used as a reference. (b) 1 km grid digital elevation model obtained from nearest neighbor (NN) coarsening of the reference 10 m grid digital elevation model. (c) 1 km grid digital elevation model obtained from NN coarsening plus depression-filling and extracted surface flow path (magenta line), as compared to the reference surface flow path (gray line). (d) 1 km grid digital elevation model obtained from compound method (CM) coarsening of the reference 10 m grid digital elevation model. (e) 1 km grid digital elevation model obtained from CM coarsening plus depression-filling and extracted surface flow path (magenta line), as compared to the reference surface flow path (gray line). (f) 1 km grid digital elevation model obtained from hydrography-driven (HD) coarsening of the reference 10 m grid digital elevation model (no depressions are generated in this case) and extracted surface flow path (magenta line) as compared to the reference surface flow path (gray line).
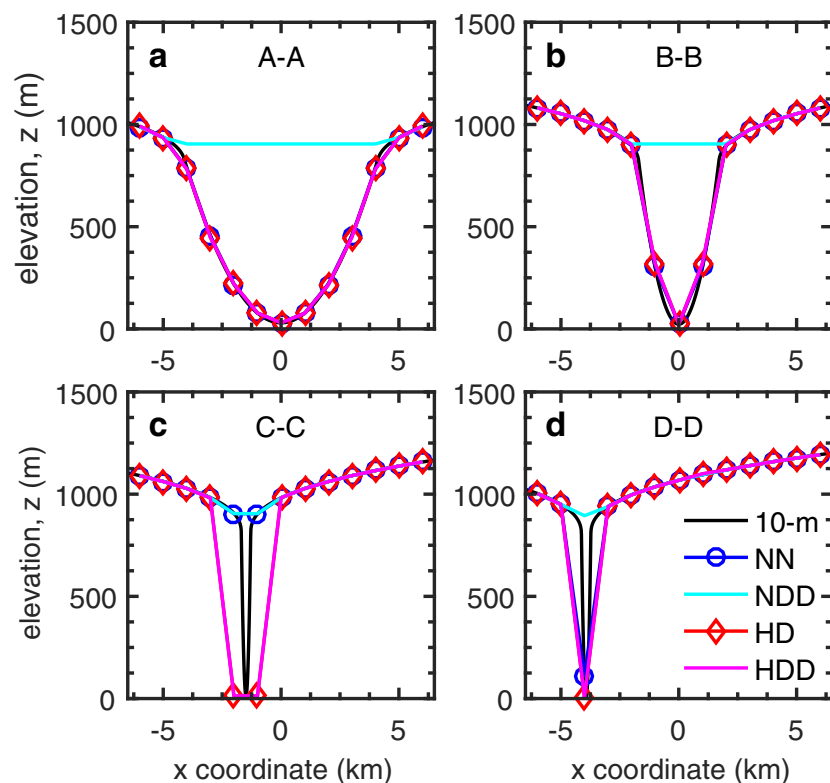

Figure 3. Valley cross sections (a) A–A, (b) B–B, (c) C–C, and (d) D–D reported in Figure 2, showing the high-resolution (10 m) topographic data and the alterations caused by nearest neighbor (NN) and hydrography-driven (HD) coarsening to the resolution of 1 km plus depression-filling (NND and HDD, respectively). No depressions are generated after the HD coarsening in the case reported in Figures 2 and 3. Results obtained from compound method (CM) coarsening (shown in Figure 2 but not in Figure 3) are similar to those obtained from NN coarsening.

$$x_t = 2000 \left[\sin \left(\frac{13,000 - y}{3000} \frac{\pi}{2} \right) - 1 \right] \tag{1}$$

for $0 \leq y < 10,000$ m. The elevation of the thalweg is set equal to $z_t = 0.0017 y$ for $0 \leq y < 20,000$ m. Around the thalweg, cross sections are assumed to display a vertical axes of symmetry passing from the thalweg, with a lower parabolic valley and upper plateaus above both sides of the parabolic valley (e.g., sections A–A and B–B in Figures 2a and 3a).

The lower parabolic valley is generated by using the functional relationship

$$z = n(x - x_t)^2 + z_t \tag{2}$$

for $x_t - \sqrt{z_p/n} \leq x \leq x_t + \sqrt{z_p/n}$ and $z_t \leq z \leq z_t + z_p$, where n is a parameter indicating the degree of narrowness of the valley, x_t is a planar coordinate of the thalweg, z_t is the elevation of the thalweg, z_p is the elevation of the point at which the plateau initiate. On the (hydrographic) right-hand side of the parabolic valley, for $x < x_t - \sqrt{z_p/n}$ and $z > z_t + z_p$, a plateau is generated through the power function relationship

$$z = z_R + 10 (x_R - x)^{0.4}, \tag{3}$$

where $z_R = z_t + z_p + 10(n z_p/4)^{-1/3}$ and $x_R = x_t - \sqrt{z_p/n} + (n z_p/4)^{-5/6}$ are determined by imposing continuity of elevation z and slope z' at $z = z_t + z_p$. On the (hydrographic) left-hand side of the parabolic valley, for $x > x_t + \sqrt{z_p/n}$ and $z > z_t + z_p$, a plateau is generated through the power function relationship

$$z = z_L + 10 (x - x_L)^{0.4}, \tag{4}$$

where $z_L = z_t + z_p + 10(n z_p/4)^{-1/3}$ and $x_L = x_t + \sqrt{z_p/n} - (n z_p/4)^{-5/6}$ are determined by imposing continuity of elevation z and slope z' at $z = z_t + z_p$. The degree of narrowness of the parabolic valley around the thalweg is imposed along the thalweg by varying coefficient n so as to obtain $n = 2 \times 10^{-2}$ m^{-1} for $5 \leq y \leq 9,995$ m, $n = 2.7417 \times 10^{-42}(19,995 - y)^{9.9658}$ m^{-1} for $10,005 \leq y \leq 14,995$ m, and $n = 0.8409(19,995 - y)^{-1.2500}$ m^{-1} for $15,005 \leq y \leq 19,995$ m. This makes it possible to generate a complex valley composed of a deep and narrow canyon for $0 \leq y \leq 10,000$ m (e.g., sections C–C and D–D in Figures 2a, 3c, and 3d) draining a wider upstream valley for $10,000 < y \leq 20,000$ m (e.g., sections A–A and B–B in Figures 2a, 3a, and 3b).

The high-resolution (10 m) grid digital elevation model of the SV is shown in Figure 2a along with the reference mainstream obtained by setting the threshold area for channel initiation A_t equal to 5×10^6 m^2. These topographic data do not display depressions or pits. The results obtained from NN coarsening to a 1 km grid are shown in Figure 2b. The digital elevation model obtained after NN coarsening plus depression-filling (NND) and the related mainstream obtained by setting $A_t = 5 \times 10^6$ m^2 are shown in Figure 2c. The results obtained from CM coarsening to a 1 km grid are shown in Figure 2d. The digital elevation model obtained after CM coarsening plus depression-filling (CMD) and the related mainstream obtained by setting $A_t = 5 \times 10^6$ m^2 are shown in Figure 2e. The results obtained from HD coarsening to a 1 km grid and the related mainstream obtained by setting $A_t = 5 \times 10^6$ m^2 are shown in Figure 2f. No depression-filling is needed in this case after HD coarsening. Cross sections A–A, B–B, C–C, and D–D observed in high-resolution data and after NN and HD coarsening and possible depression-filling are reported in Figure 3. NN and CM coarsening produce similar results (Figures 2b–2e). The case of the SV illustrated in Figures 2 and 3 reveals that NN and CM coarsening may produce local artificial damming of deep and narrow valleys (Figures 2b–2e and 3), and that these local artifacts may have significant effects on upstream drainage areas when a depression-filling procedure is applied (Figures 2c, 2e, and 3). This limitation of the NN and CM coarsening is eliminated or at least mitigated by the HD coarsening, which retains the elevation of the highest-order path within the coarse grid cell and does not cause therefore unnecessary depression-filling due to erroneous valley damming (Figures 2f and 3). The HD coarsening strategy contributes to drainage basin hydrology by simultaneously preserving channel profiles and minimizing artificial depression-filling.

3.2. Crostolo River Drainage Basin

The first real case is the Crostolo River drainage basin shown in Figure 4. The Crostolo River is a tributary of the Po River. The considered drainage basin has an extension of approximately 86 km^2 and is located in northern Italian Apennines near the town of Reggio Emilia. The centroid of the drainage basin has latitude 44°34'14.17"N and longitude 10°31'42.06"E. Planimetric and relief features of the Crostolo River drainage
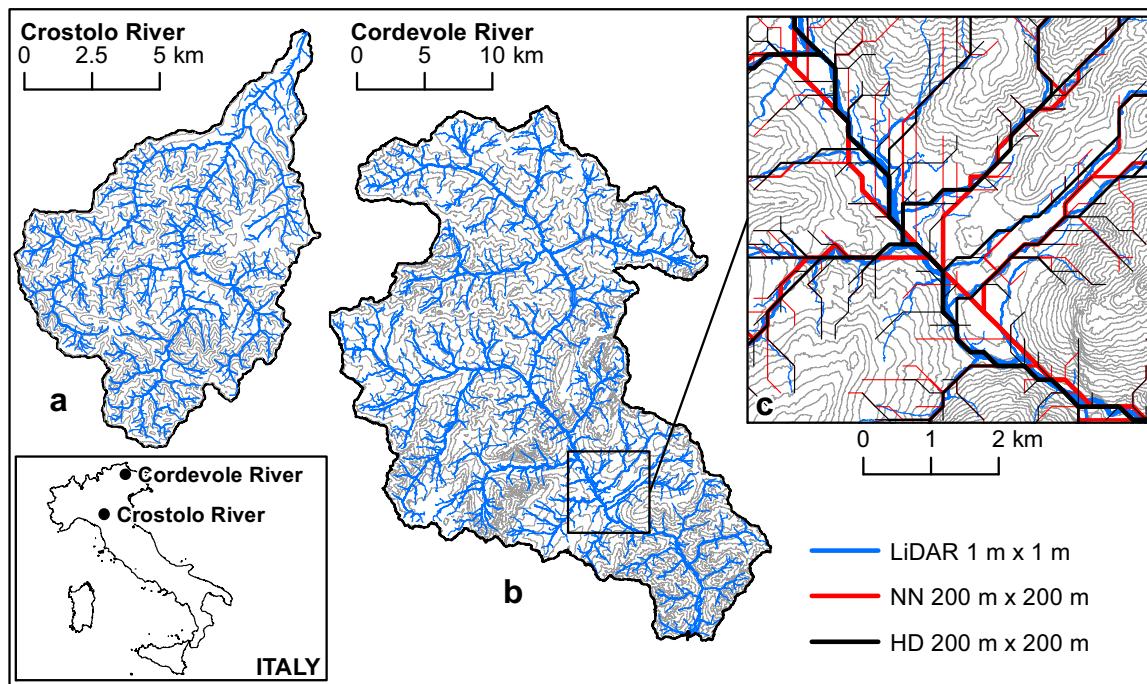
Figure 4. Channel networks in the (a) Crostolo River and (b) Cordevole River drainage basins used to test the hydrography-driven coarsening. 1 m digital elevation models generated from lidar surveys are used after depression-filling to provide reference grid and channel networks (blue lines). (c) Channel networks extracted from 200 m digital elevation models obtained after nearest neighbor (NN) coarsening and depression-filling (red lines) or hydrography-driven (HD) coarsening only (black lines) are reported in the inset that zooms in a portion of the Cordevole River drainage basin. Results obtained from compound method (CM) coarsening (not shown in Figure 4) are similar to those obtained from NN coarsening.

basin are shown in Figure 4a. The elevation ranges from 136 to 740 m above sea level (asl) with an average elevation of 391 m asl. In this area, the geologic substratum is constituted by clay shales of marine origin. Clay-rich soils are mostly covered by bush and grass but also cultivated land are common. The topography can be described as fairly complex as a result of surface water erosion and active landsliding. The Crostolo River drainage basin is selected in the present study to investigate the behavior of NN, CM, and HD coarsening in a real case where the topographic structures reproduced by the SV are not observed.

3.3. Cordevole River Drainage Basin

The second real case is the Cordevole River drainage basin shown in Figure 4. The Cordevole River is a tributary of the Piave River. The considered drainage basin has an extension of approximately 690 km² and is located in eastern Italian Alps (Italian Dolomites) near the town of Belluno. The centroid of the drainage basin has latitude 46°21′33.92″N and longitude 11°58′43.69″E. Planimetric and relief features of the Cordevole River drainage basin are shown in Figure 4b. The elevation ranges from 394 to 3,343 m asl with an average elevation of 1,655 m asl. The geological formations are mainly limestones, dolomite, marl, and sandstones that characterize the main ranges where jagged peaks and rock faces of hundreds of meters high arise from forests and grasslands. The complex geomorphology provide constrains for the formation of the channel network, that may extend in many cases along wide valley followed in a downstream direction by narrow canyons as reported in Figure 4c. The Cordevole River drainage basin is selected in the present study to investigate the behavior of the NN, CM, and HD coarsening in a real case, where the topographic structures reproduced by the SV are observed. As shown in the inset that zooms in a portion of the Cordevole River drainage basin reported in Figure 4c, the use of the HD coarsening in preference to the NN coarsening may have a significant impact on the extracted channel network as observed on a planimetric map. An even more significant impact is also expected on the description of the channel network relief as the HD coarsening is specifically designed to provide an accurate description of thalweg elevations and profiles.

3.4. Comparison Between Grid Coarsening Strategies

In addition to the analysis reported in Figures 2–4, the impact of grid coarsening on the representation of drainage basin topography is evaluated in Figure 5, where elevations obtained from NN and HD coarsening plus depression-filling are compared to those given by NN coarsening only, in Figure 6, where elevations obtained from NN and HD coarsening plus depression-filling are compared to those given by HD coarsening only, and in Table 1, where NN, CM, and HD coarsening are evaluated with special attention to the impact of depression-filling procedures. Grid resolutions of 10, 20, 50, 100, 200, 500, and 1,000 m are considered for the SV (Figures 5a–5f and 6a–6c and Table 1). Grid resolutions of 1, 10, 50, 100, 200, 400, and 800 m are considered for the Crostolo River and Cordevole River drainage basins (Figures 5g–5r and 6d–6i, and Table 1). It is remarked here that the elevation of a coarse grid cell obtained from the NN coarsening only, $z^{(NN)}$, is the elevation of the coarse grid cell center observed in high-resolution topographic data (e.g., point C in Figure 1), whereas the elevation of a coarse grid cell obtained from the HD coarsening only, $z^{(HD)}$, is considered in the present study to be the hydrographically most significant elevation among those observed in high-resolution topographic data within the coarse grid cell (e.g., point P in Figure 1). The elevation of a coarse grid cell obtained from the CM coarsening only, $z^{(CM)}$, is the elevation of the coarse grid cell center observed in the drainage-constrained TIN. Elevations $z^{(CM)}$ and $z^{(CMD)}$ are not reported in Figures 5 and 6.

In the perspective mentioned above, the accuracy of the elevations assigned to coarse grid cells after NN coarsening plus depression-filling (NND), namely $z^{(NND)}$, or after HD coarsening plus depression-filling (HDD), namely $z^{(HDD)}$, is evaluated by considering the elevations obtained from the HD coarsening only, namely $z^{(HD)}$, as targets. Three evaluation metrics are used, namely the mean error

$$ME = \frac{1}{N} \sum_{k=1}^{N} \epsilon_k, \tag{5}$$

the mean absolute error

$$MAE = \frac{1}{N} \sum_{k=1}^{N} |\epsilon_k|, \tag{6}$$

and the root mean square error

$$RMSE = \sqrt{\frac{1}{N} \sum_{k=1}^{N} \epsilon_k^2}, \tag{7}$$

where N is the number of coarse grid cells over which the error functions are computed, k is the counter of the grid cell, $\epsilon_k = z_k^{(NND)} - z_k^{(HD)}$ when the nearest neighbor coarsening plus depression-filling (NND) is evaluated or $\epsilon_k = z_k^{(HDD)} - z_k^{(HD)}$ when the hydrography-driven coarsening plus depression-filling (HDD) is evaluated ($k = 1, \ldots, N$). Computed values of ME, MAE, and RMSE for the SV, the Crostolo River drainage basin, and the Cordevole River drainage basin are reported in Figures 6a–6c, 6d–6f, and 6g–6j, respectively.

The impacts of the NN, CM, and HD coarsening on the representation of drainage basin topography are also evaluated in terms of altered cells (AC), percentage of altered cells (PAC), out-of-range cells (OORC), and percentage of out-of-range cells (POORC) as reported in Table 1. AC is the number of coarse grid cells displaying altered elevations after depression-filling with respect to the elevations assigned after NN, CM, or HD coarsening only, namely $z^{(NND)} \neq z^{(NN)}$, $z^{(CMD)} \neq z^{(CM)}$, or $z^{(HDD)} \neq z^{(HD)}$, respectively (Figure 1). PAC is the percentage of AC with respect to the total number of coarse grid cells in the drainage system. OORC is the number of coarse grid cells displaying elevations that are outside the elevation range observed within these coarse grid cells in high-resolution topographic data, namely $z^{(NND)} > z^{(max)}$, $z^{(CMD)} < z^{(min)}$ or $z^{(CMD)} > z^{(max)}$, or $z^{(HDD)} > z^{(max)}$, respectively (Figure 1). POORC is the percentage of OORC with respect to the total number of coarse grid cells in the drainage system.

A further evaluation of the impact of grid coarsening on the representation of drainage basin topography is obtained by considering the sample distributions Z of the elevations observed in high-resolution topographic data and in coarse-resolution digital elevation models after NN, CM, and HD coarsening plus depression-filling. Special attention is focused on grid cells lying along the drainage system mainstreams.
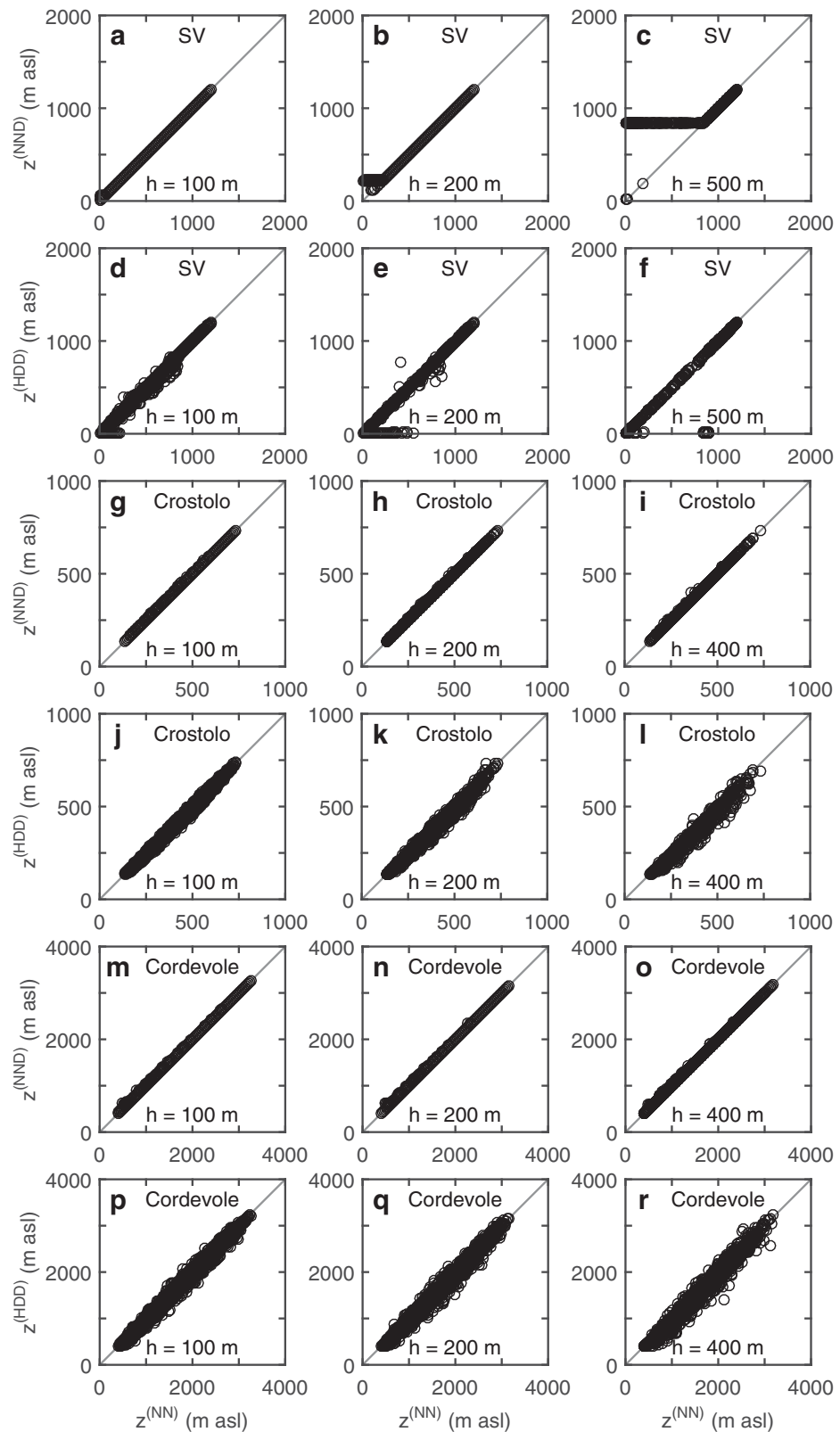
Figure 5. Comparison between nearest neighbor (NN) and hydrography-driven (HD) coarsening in the cases of (a–f) the synthetic valley (SV), (g–l) the Crostolo River drainage basin, and (m–r) the Cordevole River drainage basin (Figures 2 and 4). Grid cell elevations obtained from nearest neighbor coarsening and depression-filling, $z^{(NND)}$, or from hydrography-driven coarsening and depression-filling, $z^{(HDD)}$, are plotted against the grid cell elevations obtained from nearest neighbor coarsening only, $z^{(NN)}$.
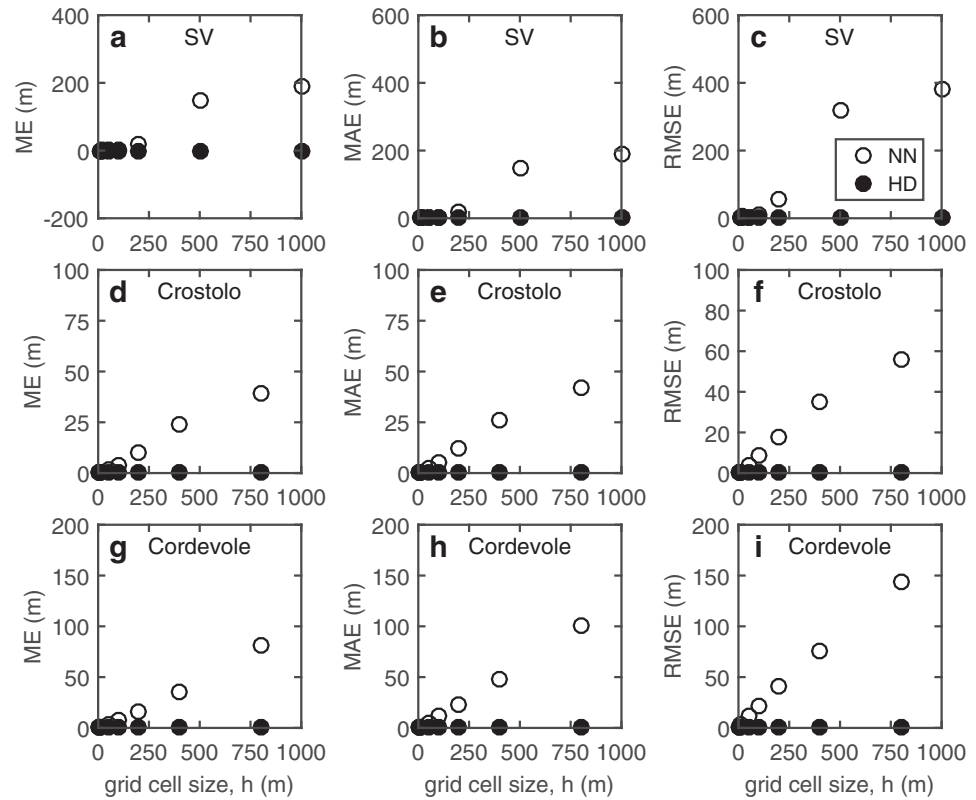
Figure 6. Mean error (ME), mean absolute error (MAE), and root mean square error (RMSE) displayed by the nearest neighbor (NN) and hydrography-driven (HD) coarsening in the cases of (a–c) the synthetic valley, (d–f) the Crostolo River drainage basin, and (g–i) the Cordevole River drainage basin. Errors are evaluated with respect to the elevation $z_k^{(HD)}$ as $\epsilon_k = z_k^{(NND)} - z_k^{(HD)}$, in the case of the nearest neighbor coarsening plus depression-filling, or $\epsilon_k = z_k^{(HDD)} - z_k^{(HD)}$, in the case of the hydrography-driven coarsening plus depression-filling.

The distributions of elevations observed along the mainstreams of the SV, the Crostolo River drainage basin, and the Cordevole River drainage basin are reported in Figures 7a–7c, 7d–7f, and 7g–7j, respectively, in terms of cumulative density functions (CDF). The entropy of grid cell elevations is used to provide a measure of the diversification of possible elevations (i.e., the internal states) that surface water elements can take on the land surface of the drainage system (i.e., the whole system). The higher is the entropy of elevations, the higher is the diversity of the represented land surface topography. The differential entropy $s(Z)$ of the continuous distribution Z representing the elevations z observed in the drainage system or along the drainage system mainstream is defined as

$$s(Z) = -\int_{\mathcal{Z}} f(z) \, \log f(z) \, dz, \tag{8}$$

where $\mathcal{Z}$ is the support set of the distribution Z, namely the elevation range in the drainage system or along the drainage system mainstream, $f(z)$ is the probability density function (PDF) of Z, namely $f(z) = dF(z)/dz$, $F(z)$ being the CDF of Z, and "log" denotes the natural (base e) logarithm (Cover & Thomas, 2006, p. 243). By dividing the range $\mathcal{Z}$ of the sample distributions Z into N bins of length Δ, the entropy of Z can be computed as

$$S(Z, \Delta) = -\sum_{i=1}^{N} p_i \log p_i, \tag{9}$$

where

$$p_i = \int_{(i-1)\Delta}^{i\Delta} f(z) \, dz \tag{10}$$

or, equivalently, $p_i = F(i\Delta) - F((i-1)\Delta)$ $(i = 1, \ldots, N)$.

Table 1
Cells Displaying Elevation Altered by Depression-Filling and Cells Displaying Out-of-Range Elevation in the Considered Test Cases[a]

	Nearest neighbor coarsening				Compound method coarsening[b]				Hydrography-driven coarsening			
h (m)	AC (cells)	PAC (%)	OORC (cells)	POORC (%)	AC (cells)	PAC (%)	OORC (cells)	POORC (%)	AC (cells)	PAC (%)	OORC (cells)	POORC (%)
Synthetic valley ($A = 2.603$ km^2)												
10[c]	0	0.0	0	0.0	0	0.0	0	0.0	0	0.0	0	0.0
20	473	0.1	0	0.0	1,567	0.2	451,481	69.6	15	0.0	0	0.0
50	832	0.8	557	0.5	759	0.7	54,780	53.0	0	0.0	0	0.0
100	1,180	4.6	977	3.8	1,177	4.6	7,145	27.8	0	0.0	0	0.0
200	714	11.0	587	9.0	712	11.0	1,139	17.5	0	0.0	0	0.0
500	237	24.3	176	18.1	237	24.3	176	18.1	0	0.0	0	0.0
1,000	70	26.9	42	16.2	71	27.3	40	15.4	0	0.0	0	0.0
Crostolo River drainage basin ($A = 85.772$ km^2)												
1[c]	0	0.0	0	0.0	0	0.0	0	0.0	0	0.0	0	0.0
10	4,026	0.5	553	0.1	5,473	0.6	17,479	2.0	34	0.0	11	0.0
50	423	1.2	1	0.0	464	1.4	64	0.2	0	0.0	0	0.0
100	150	1.7	0	0.0	155	1.8	6	0.1	1	0.0	0	0.0
200	55	2.6	0	0.0	59	2.8	0	0.0	0	0.0	0	0.0
400	26	4.8	0	0.0	26	4.8	0	0.0	0	0.0	0	0.0
800	13	9.5	0	0.0	13	9.5	0	0.0	0	0.0	0	0.0
Cordevole River drainage basin ($A = 690.804$ km^2)												
1[c]	0	0.0	0	0.0	0	0.0	0	0.0	0	0.0	0	0.0
10	27,480	0.4	11,535	0.2	34,755	0.5	273,332	4.0	149	0.0	146	0.0
50	1,536	0.6	129	0.0	1,760	0.6	822	0.3	11	0.0	0	0.0
100	834	1.2	193	0.3	840	1.2	219	0.3	1	0.0	0	0.0
200	377	2.2	102	0.6	380	2.2	103	0.6	0	0.0	0	0.0
400	122	2.8	3	0.1	124	2.9	3	0.1	0	0.0	0	0.0
800	75	6.9	10	0.9	76	7.0	10	0.9	0	0.0	0	0.0

[a]h: grid cell size; AC: altered cells; PAC: percentage of altered cells; OORC: out-of-range cells; and POORC: percentage of out-of-range cells. [b]Parameter Z-tolerance is set equal to 8.0, 0.8, and 3.0 m for the SV, the Crostolo River drainage basin, and the Cordevole River drainage basin, respectively (see Chen et al., 2012, value 3.0 m due to ArcGIS computational limitations). [c]Grid cell size in the reference digital elevation model.

As shown in Cover and Thomas (2006, p. 248), $S(Z, \Delta) + \log \Delta \rightarrow s(Z)$ as $\Delta \rightarrow 0$, which indicates a useful rule for estimating the value of $s(Z)$ given by equation (8) from the sample distributions reported in Figure 7. In the present study, for values of Δ ranging from 1 to 50 m, the differential entropy of elevations given by

$$s(Z) = S(Z, \Delta) + \log \Delta \tag{11}$$

is found to be essentially invariant with Δ. The percentage change in the differential entropy of elevations observed when coarsening high-resolution topographic data to coarse-resolution grid digital elevation models is computed as

$$\delta s = \frac{s(Z^{(CR)}) - s(Z^{(HR)})}{s(Z^{(HR)})} \times 100, \tag{12}$$

where $s(Z^{(CR)})$ and $s(Z^{(HR)})$ are the values of differential entropy of elevations computed over coarse-resolution (CR) and high-resolution (HR) grid digital elevation models, respectively. CR grid digital elevation models are obtained from NN, CM, or HD coarsening plus depression-filling. HR grid digital elevation models have resolutions of 10 m for the SV and 1 m for the Crostolo River and Cordevole River drainage basins. The values of differential entropy of elevations s and of the related percentage change in differential entropy of elevations δs caused by coarsening plus depression-filling are computed by using equations (11) and (12), respectively, with $\Delta = 30$ m and reported in Table 2. As also made in the analysis reported in Figure 7, special attention is focused in Table 2 on the elevations of grid cells lying along the drainage system mainstreams.
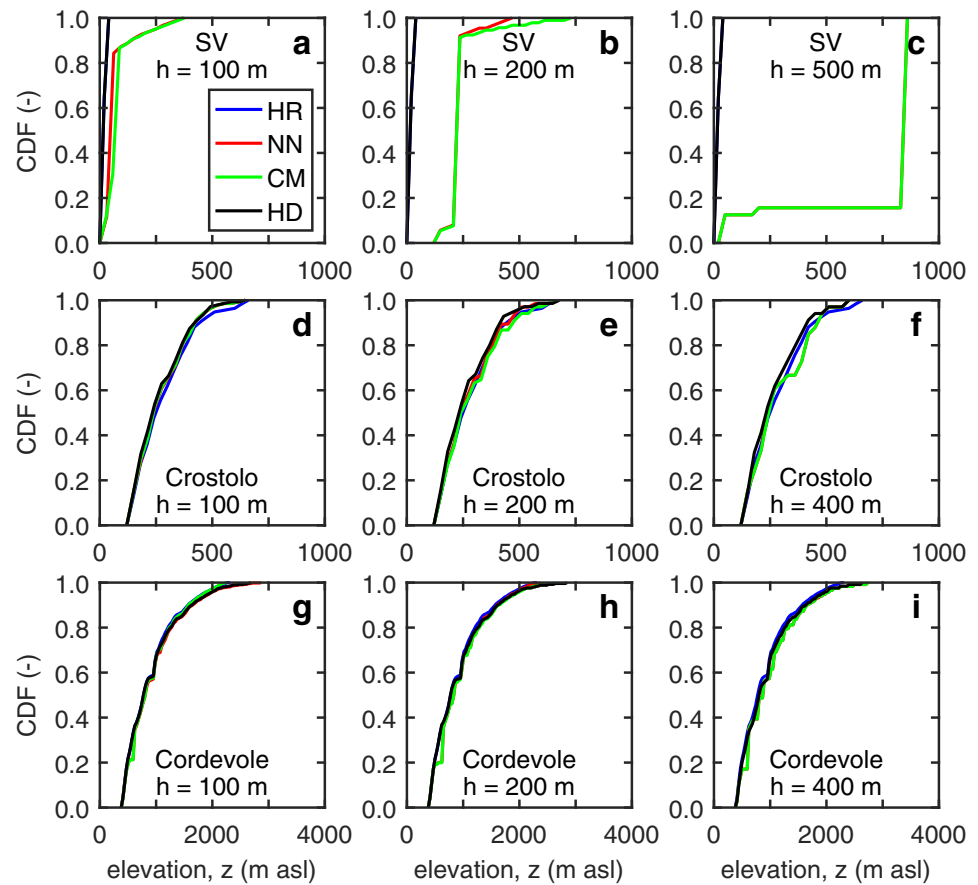
Figure 7. Cumulative density function (CDF) of the elevations observed, in high-resolution (HR) topographic data and in digital elevation models obtained from nearest neighbor (NN), compound method (CM), and hydrography-driven (HD) coarsening, along the mainstreams of (a–c) the synthetic valley (SV), (d–f) the Crostolo River drainage basin, and (g–i) the Cordevole River drainage basin.

3.5. Evaluation of Extracted Surface Flow Paths

Additional metrics are defined to evaluate the ability of coarsening methods to provide consistent surface flow paths with respect to those observed in high-resolution digital elevation models. It is remarked here that in the present study the focus is not on depression-filling and slope direction methods, but rather on the coarsening strategies used to retain the information content of high-resolution data in coarsened digital elevation models. The results obtained from the proposed HD coarsening are compared to those obtained from NN and CM coarsening.

The impact of the coarsening strategy on the plan geometry of extracted surface flow paths is expressed by the mean plan distance

$$\text{MPD} = \frac{1}{N} \sum_{k=1}^{N} d_k, \tag{13}$$

the mean absolute plan distance

$$\text{MAPD} = \frac{1}{N} \sum_{k=1}^{N} |d_k|, \tag{14}$$

and the root mean square plan distance

$$\text{RMSPD} = \sqrt{\frac{1}{N} \sum_{k=1}^{N} d_k^2}, \tag{15}$$

where N is the number of coarse grid cells of the evaluated surface flow path and

Table 2
Baseline and Percentage Change in Entropy of Elevations in the Considered Test Cases[a]

| | Nearest neighbor coarsening | | | | Compound method coarsening[b] | | | | Hydrography-driven coarsening | | | |
| | Drainage system | | Mainstream | | Drainage system | | Mainstream | | Drainage system | | Mainstream | |
h (m)	s (–)	δs (%)	s (–)	δs (%)	s (–)	δs (%)	S (–)	δs (%)	s (–)	δs (%)	s (–)	δs (%)
Synthetic valley (A = 2.603 km²)												
10[c]	6.51	0.00	4.05	0.00	6.51	0.00	4.05	0.00	6.51	0.00	4.05	0.00
20	6.51	0.02	4.05	−0.01	6.49	−0.26	4.09	0.82	6.51	0.05	4.05	−0.11
50	6.49	−0.32	4.45	9.70	6.49	−0.33	3.40	−16.10	6.52	0.06	4.05	−0.14
100	6.45	−1.01	4.53	11.66	6.45	−1.02	4.87	20.05	6.52	0.12	4.05	−0.12
200	6.29	−3.42	4.17	2.81	6.27	−3.73	4.20	3.60	6.51	−0.09	4.04	−0.23
500	5.75	−11.70	3.91	−3.48	5.73	−12.08	3.91	−3.48	6.47	−0.62	4.05	0.00
1,000	5.58	−14.31	3.40	−16.10	5.57	−14.45	3.40	−16.10	6.31	−3.15	4.05	−0.13
Crostolo River drainage basin (A = 85.772 km²)												
1[c]	6.24	0.00	5.98	0.00	6.24	0.00	5.98	0.00	6.24	0.00	5.98	0.00
10	6.24	0.00	5.96	−0.33	6.24	−0.00	5.91	−1.17	6.24	−0.00	5.97	−0.25
50	6.21	−0.53	5.91	−1.16	6.21	−0.54	5.90	−1.39	6.21	−0.54	5.90	−1.46
100	6.21	−0.52	5.87	−1.85	6.21	−0.52	5.86	−2.09	6.24	−0.02	5.84	−2.36
200	6.20	−0.63	5.83	−2.60	6.20	−0.64	5.89	−1.57	6.20	−0.70	5.81	−2.81
400	6.20	−0.64	5.78	−3.41	6.20	−0.65	5.79	−3.18	6.18	−0.92	5.81	−2.78
800	6.20	−0.69	5.33	−10.89	6.20	−0.60	5.44	−9.05	6.14	−1.65	5.68	−4.96
Cordevole River drainage basin (A = 690.804 km²)												
1[c]	7.64	0.00	7.09	0.00	7.64	0.00	7.09	0.00	7.64	0.00	7.09	0.00
10	7.64	0.00	7.12	0.42	7.64	−0.00	7.09	−0.10	7.64	−0.00	7.12	0.34
50	7.64	−0.00	7.09	−0.07	7.64	−0.01	6.91	−2.63	7.64	0.09	7.12	0.31
100	7.64	−0.02	7.00	−1.39	7.63	−0.07	6.93	−2.32	7.64	−0.03	7.15	0.75
200	7.63	−0.12	6.74	−4.98	7.63	−0.12	6.81	−3.99	7.65	0.13	7.09	−0.09
400	7.63	−0.13	6.53	−7.98	7.63	−0.13	6.53	−7.98	7.66	0.24	7.09	−0.08
800	7.52	−1.54	5.89	−17.01	7.52	−1.58	5.89	−17.01	7.65	0.16	6.81	−4.03

[a]h: grid cell size; s: differential entropy of elevations computed from equation (11) with Δ = 30 m; δs: percentage change in s computed from equation (12). [b]Parameter Z-tolerance is set equal to 8.0, 0.8, and 3.0 m for the SV, the Crostolo River drainage basin, and the Cordevole River drainage basin, respectively (see Chen et al., 2012, value 3.0 m due to ArcGIS computational limitations). [c]Grid cell size in the reference digital elevation model.

$$d_k = \pm \sqrt{\left(x_k^{(C)} - x_k^{(P)}\right)^2 + \left(y_k^{(C)} - y_k^{(P)}\right)^2} \tag{16}$$

is the elemental distance between the coarse grid cell center C lying along the evaluated flow path and the closest point P of the flow path used as a reference as sketched in Figure 8 ($k = 1, \ldots, N$). The value of the distance d_k ($k = 1, \ldots, N$) in equation (16) is considered to be positive when the cell center C lies on the right-hand side of an observed traveling downslope along the reference surface flow path, null when it lies on the reference flow path, and negative when it lies on the left-hand side of the reference surface flow path. Details on the computation of the elemental distances d_k ($k = 1, \ldots, N$) can be found in Orlandini et al. (2014). Computed values of MPD, MAPD, and RMSPD for the SV, the Crostolo River drainage basin, and the Cordevole River drainage basin are reported in Figures 9a–9c, 9g–9i, and 9m–9o, respectively.

The impact of the coarsening strategy on the relief of extracted surface flow paths is expressed by the mean elevation drop

$$\text{MED} = \frac{1}{N} \sum_{k=1}^{N} e_k, \tag{17}$$

the mean absolute elevation drop

$$\text{MAED} = \frac{1}{N} \sum_{k=1}^{N} |e_k|, \tag{18}$$
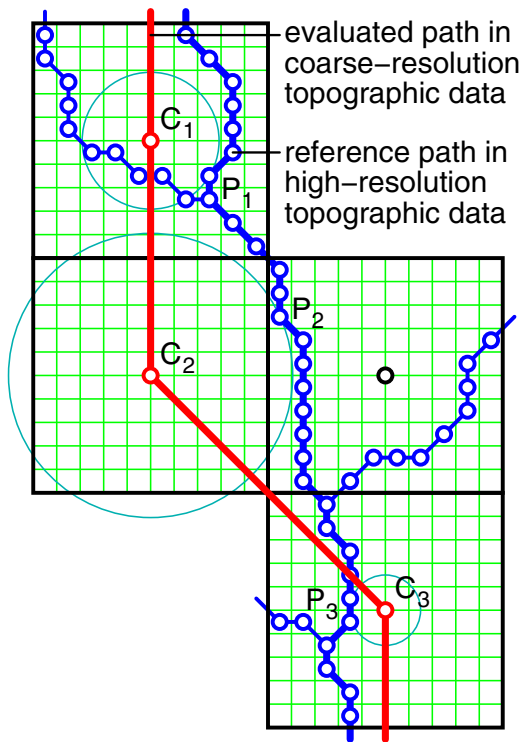
and the root mean square elevation drop

Figure 8. Sketch of the comparison between surface flow paths extracted in the coarse-resolution grid (red line) and in the high-resolution grid (blue line). Surface flow paths having the same Horton order are compared along their full extension. For any coarse-resolution grid cell center (C_1, C_2, and C_3 in Figure 8) the closest point lying on the reference surface flow path extracted in the high-resolution grid is identified (P_1, P_2, and P_3 in Figure 8). The plan distance between points C_i and points P_i ($i=1,2,\ldots$) and the elevation drops between the same points are used to compute the evaluation metrics introduced in section 3.

$$\mathrm{RMSED} = \sqrt{\frac{1}{N}\sum_{k=1}^{N} e_k^2}, \qquad (19)$$

where N is the number of coarse grid cells of the evaluated surface flow path and

$$e_k = z_k^{(C)} - z_k^{(P)} \qquad (20)$$

is the elemental drop between the coarse grid cell center C lying along the evaluated flow path and the closest point P of the flow path used as a reference as sketched in Figure 8 ($k=1,\ldots,N$). For any coarse grid cell center C, the closest point P used in equations (17–19) may be internal to the coarse grid cell as it occurs, for instance, in the case of points C_1 and P_1 reported in Figure 8, or it may rather be external to the coarse grid cell as occurs, for instance, in the case of points C_2 and P_2 reported in Figure 8. It is also noted that the computation of the distance d_k ($k=1,\ldots,N$) in equations (13–16) may involve the center C of the coarse grid cell lying along the evaluated surface flow path and the closest center P of the high-resolution cell lying along the reference surface flow path as occurs, for instance, in the case of point P_1 reported in Figure 8, or may rather involve a point P of the reference flow path which is not a cell center as occurs, for instance, in the case of point P_3 reported in Figure 8. Computed values of MED, MAED, and RMSED for the SV, the Crostolo River drainage basin, and the Cordevole River drainage basin are reported in Figures 9d–9f, 9j–9l, and 9p–9r, respectively.

4. Discussion

The HD coarsening strategy proposed in the present study is based on the assumption that the elevation $z^{(HD)}$ defined in section 2.3 and in Figure 1 is the hydrographically most significant elevation observed in high-res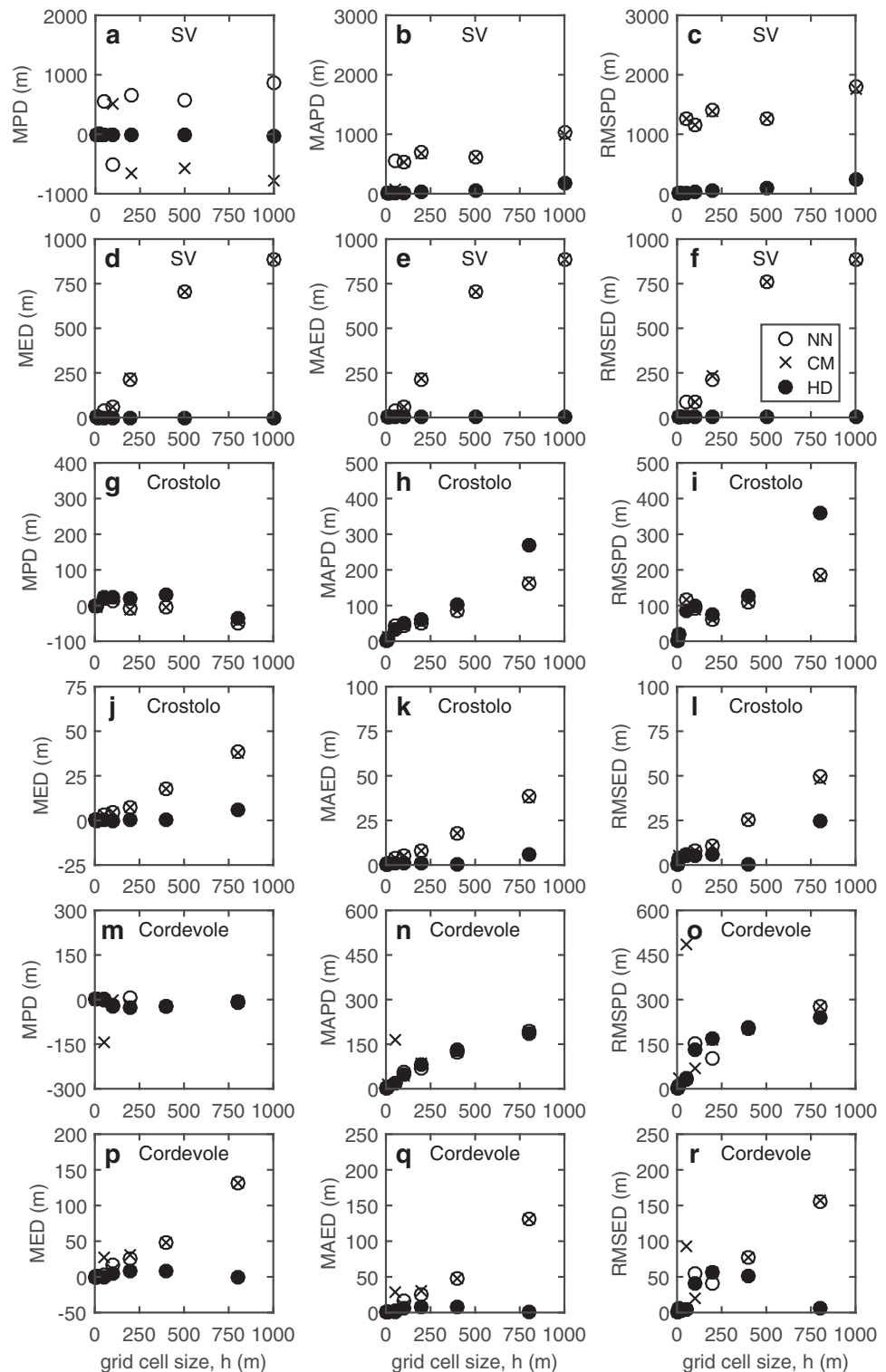olution topographic data within the coarse grid cell. Points "P" introduced in Figure 1 are the closest points to the coarse grid cell centers "C" that retain the essential information about the highest-order path observed within the coarse grid cell. With respect to NN coarsening, points "P" preserve planimetric significance since they are as close as possible to the grid cell centers "C," and they convey a greater relief significance since they provide the thalweg elevation at which the water actually flows in the highest-order path observed. As illustrated in Figures 2 and 3 for the SV, when high-resolution topographic data describing a narrow canyon are coarsened by using standard NN coarsening, the information loss regarding thalweg elevation (Figures 2b, 3c, and 3d) yields local artifacts and abnormal depression-filling in upstream areas (Figures 2c, 2d, 3a, and 3b). The elevation $z^{(HD)}$ used in the HD coarsening is hydrographically more significant than the elevation $z^{(NN)}$ used in the NN coarsening because it provides a better description of the profiles of surface flow paths with direct implications on the description of land surface topography due to the reduction of the impact of depression-filling. The results reported in Table 1 clearly indicate that the need for depression-filling in coarse-resolution digital elevation models is eliminated or at least drastically reduced when the HD coarsening is used in preference to NN and CM coarsening. In absolute terms, the results reported in Figures 2 and 3, combined with those reported in Table 1, reveal the ability of the HD coarsening strategy to preserve the thalweg profile of the SV observed in high-resolution topographic data and to reduce the impact of depression-filling to null or insignificant levels.

The results reported in Table 1 also reveal that the number of out-of-range cells, OORC, may be greater than the number of altered cells, AC, when the CM coarsening is used and a small grid cell size h of the coarse digital elevation model is selected. In these cases, at least OORC$-$AC coarse grid cells in the drainage system are out-of-range as a result of coarsening only, and not of depression-filling. In fact, the TIN

Figure 9. Mean plan distance (MPD), mean absolute plan distance (MAPD), root mean square plan distance (RMSPD), mean elevation drop (MED), mean absolute elevation drop (MAED), and root mean square elevation drop (RMSED) displayed by the nearest neighbor (NN), compound method (CM), and hydrography-driven (HD) coarsening in the cases of (a–f) the synthetic valley, (g–l) the Crostolo River drainage basin, and (m–r) the Cordevole River drainage basin.

generated in the CM coarsening by setting a given Z-tolerance, shortly denoted as Z_t, provides for each coarse grid cell an elevation that falls in the range between $z^{(min)}$ and $z^{(max)}$ if $z^{(NN)} - Z_t \geq z^{(min)}$ and $z^{(NN)} + Z_t \leq z^{(max)}$, or equivalently if $Z_t \leq z^{(NN)} - z^{(min)}$ and $Z_t \leq z^{(max)} - z^{(NN)}$, or roughly if $Z_t \leq (z^{(max)} - z^{(min)})/2$ by assuming that $z^{(NN)}$ is centered between $z^{(min)}$ and $z^{(max)}$ (Figure 1). Cases contributing to OORC may instead occur if $Z_t > z^{(NN)} - z^{(min)}$ or $Z_t > z^{(max)} - z^{(NN)}$, or more restrictively if $Z_t > z^{(max)} - z^{(min)}$. These statements are confirmed by the applications of the CM coarsening reported in the present study. NN and CM coarsening are found to be similar when high-resolution digital elevation models are coarsened to large grid cells ($h \geq 500$ m for the SV, $h \geq 100$ m for the Crostolo and Cordevole River drainage basins, as reported in Tables 1 and 2, and in Figures 2, 7, and 9). Under these conditions, the TIN generated in the CM coarsening describes accurately valley and channel thalwegs observed in high-resolution topographic data with no need for a drainage-constrained TIN, and also describes accurately the topography of coarse grid cells displaying elevation ranges $z^{(max)} - z^{(min)}$ significantly greater than Z-tolerance. The coarse digital elevation model generated from this TIN is therefore close to the one generated directly from high-resolution topographic data by using the NN coarsening. It is also confirmed that CM coarsening may be less accurate than NN coarsening when high-resolution digital elevation models are coarsened to small grid cells ($h < 500$ m for the SV, $h < 100$ m for the Crostolo and Cordevole River drainage basins, as reported in Table 1 and Figure 9). Under these conditions, the TIN generated in the CM coarsening may be unable to describe accurately the topography of many coarse grid cells, including those displaying elevation ranges $z^{(max)} - z^{(min)}$ less than Z-tolerance. The results reported in Table 1 reveal that CM coarsening is less accurate than NN coarsening for small values of h and essentially equivalent to NN coarsening for large values of h. While NN coarsening preserves the elevations of the high-resolution topographic data at the centers of coarse grid cells, and the HD coarsening uses the elevations of the hydrographically most significant points observed within the coarse grid cells, the CM coarsening may not display neither the former nor the latter quality.

Coarse-resolution grid cell elevations $z^{(NND)}$ and $z^{(HDD)}$ given by the NN coarsening plus depression-filling (NND) and HD coarsening plus depression-filling (HDD) are compared to the elevations $z^{(NN)}$ obtained from NN coarsening only as reported in Figure 5. The case of the SV highlights how NN coarsening may cause an abnormal impact of depression-filling procedures as a result of erroneous damming of valleys ($z^{(NND)} \gg z^{(NN)}$ in Figures 5b and 5c). The HD coarsening may provide different elevations of coarse grid cells with respect to those provided by NN coarsening especially where the thalweg of the highest-order surface flow path is not close to the coarse grid cell center ($z^{(HDD)} > z^{(NN)}$ or $z^{(HDD)} < z^{(NN)}$ in Figures 5d–5f), but it significantly mitigates the effects of depression-filling by preventing erroneous damming of canyons (Figures 5a–5f). In the most regular portions of the SV (lateral areas draining into the canyon), the HD coarsening is found to provide elevations $z^{(HDD)}$ close to $z^{(NN)}$ indicating that differences between the coarsening strategies examined can especially be expected in steep complex terrains. The real cases of the Crostolo River and Cordevole River drainage basins reveal that the effects highlighted in the SV may attenuate when real drainage basins are examined (Figures 5g–5r). The HD coarsening plus depression-filling displays greater deviations ($z^{(HDD)} - z^{(NN)}$) than those displayed by NN coarsening plus depression-filling ($z^{(NND)} - z^{(NN)}$), indicating that the deviations due to the consideration of points "P" in preference to points "C" within the coarse grid cell may dominate over those caused by erroneous depression-filling (Figures 5g–5r).

The elevations $z^{(HD)}$ provided by the HD coarsening are, however, hydrographically significant and it is therefore meaningful to consider these elevations as targets. In this perspective, the elevations $z^{(HD)}$ of the points "P" are considered to be a reference in the evaluation metrics ME, MAE, and RMSE given by equations (5–7). The variations of these metrics with grid cell size h reported in Figure 6 reveal that depression-filling has an insignificant impact on coarsened data obtained from HD coarsening. This is also confirmed by the analysis reported in Table 1, where it is clearly shown that the impact of depression-filling is reduced to null or insignificant levels when the HD coarsening is applied in preference to the NN and CM coarsening. Table 1 also confirms that depression-filling plays a relatively greater role in the case of the SV than in the real cases of the Crostolo River and Cordevole River drainage basins. In any case, the relative deviation between the metrics obtained from NN and HD coarsening is found to increase with h in all the test cases. The proposed HD coarsening is therefore found to be especially relevant when high-resolution data are coarsened to relatively large cells as normally occurs in detailed, large-scale, and/or long-term hydrologic modeling. Under these conditions, CM and NN coarsening provide similar results. While the results reported in Figures

5 and 6, as well as in Table 1, do not provide a test for the NN, CM, and HD coarsening strategies but rather a comparison between methods, the results reported in Figure 7 and Table 2 provide a meaningful statistical evaluation of the obtained coarse-resolution digital elevation models with respect to the original high-resolution topographic data.

For all the SV, the Crostolo River drainage basin, and the Cordevole River drainage basin, the CDF of elevations obtained from HD coarsening plus depression-filling is significantly closer to the CDF of elevations observed in high-resolution topographic data after depression-filling than the CDF of elevations obtained from NN coarsening plus depression-filling, with relative differences increasing as the size of the coarse grid cell increases (Figures 7c, 7f, and 7i). Results obtained from CM coarsening are shown in Figure 7 to be similar to those obtained from NN coarsening. The values of differential entropy of elevations, s, reported in Table 2 reveal that in the case of the SV the HD coarsening offers a remarkably better ability than the NN and CM coarsening to preserve the information content of high-resolution topographic data (i.e., a smaller percentage reduction in the entropy of elevations, $-\delta s$). This is observed when the entropy of elevations is computed over the whole drainage system and also, to a greater extent, when the attention is focused on the SV mainstream. The percentage reduction in the differential entropy of elevations with respect to the reference case obtained by considering high-resolution topographic data, $-\delta s$, increases rapidly as the size of the coarse grid cell increases. The same evidence is generally observed, even though in a less remarkable manner, over the real cases of the Crostolo River and Cordevole River drainage basins. An exception is the case of the Crostolo River drainage basin when the whole drainage system is considered. The analysis of coarse-resolution grid digital elevation models in terms of entropy of elevations confirms the greater ability of the HD coarsening strategy to preserve the information content of high-resolution topographic data as compared to the NN and CM coarsening strategies, with larger differences observed as the size of the coarse grid cell increases. The different values of percentage reduction in the entropy of elevations, $-\delta s$, observed when the whole drainage system is considered or when only the mainstream is considered suggest that further work is needed to provide an accurate representation of hill slopes within the coarse grid cells.

The NN, CM, and HD coarsening strategies are definitively tested by comparing extracted channels after coarsening and depression-filling to the corresponding channels observed in high-resolution topographic data. Plan geometry and relief of the compared channels are evaluated by computing the evaluation metrics MPD, MAPD, and RMSPD given by equations (13–15), and the evaluation metrics MED, MAED, and RMSED given by equations (17–19), respectively. As sketched in Figure 8, evaluated surface flow paths (points "C") are compared with the corresponding surface flow path observed in the high-resolution topographic data (points "P"), and not to the highest-order path observed in the coarse grid cell as made in Figure 1. The evaluation metrics are computed in the present study by considering the mainstream channel only in the considered drainage systems. A more comprehensive comparison between channel networks will be provided in a future companion investigation. The results reported in Figure 9 reveal that the plan geometry of the surface flow paths may be significantly affected by the coarsening strategy adopted in specific cases like the SV, where an incorrect representation of thalweg profile yields significant terrain alterations during the depression-filling phase (Figures 9a–9c). In real cases, the use of the HD coarsening in preference to the NN and CM coarsening does not alter generally the accuracy with which the plan geometry of channels is reproduced (Figures 9g–9i and 9m–9o). The HD coarsening yields planimetrically comparable surface flow paths to those obtained after NN and CM coarsening when the deviation from the coarse grid cell centers "C" due to the selection of points "P" is compensated by a more accurate description of surface flow path profiles, or planimetrically improved surface flow paths, when the better description of surface flow path profiles plays a critical role (Figures 2c, 2d, and 4c). More importantly, the elevation metrics focusing on relief reveal a significantly greater ability of the HD coarsening, as compared to NN and CM coarsening, to retain an accurate description of thalweg profiles and to reduce the impact of depression-filling (Figures 9d–9f, 9j–9l, and 9p–9r). In absolute terms, the results reported in Figure 9 reveal the ability of the HD coarsening strategy to provide planar descriptions of channels that are affected by acceptable absolute errors (MAPD $< h/2$ in Figures 9b, 9h, and 9n) and descriptions of channel profiles that are normally affected by insignificant absolute errors (MAED < 0.18 m, MAED < 6.00 m, and MAED < 7.92 m in Figures 9e, 9k, and 9q, respectively), over the whole range of geomorphological settings and grid cell sizes investigated.

The proposed HD coarsening strategy implemented in Fortran 90 can process the 1 m digital elevation model of the 690.804 km^2 Cordevole River drainage basin (690,803,828 cells) on a Dell workstation with

Intel Xeon E5 10 cores @3.1 GHz, 128 GB RAM with CPU times less than 3 min. For the same test case, the NN coarsening implemented in ArcGIS takes about 4 min, and the CM coarsening implemented in ArcGIS takes about 90 min.

5. Conclusions

The proposed HD coarsening strategy was shown to greatly outperform the standard NN coarsening strategy and the more complex CM coarsening strategy in synthetic test cases where coarse grid cells are used to describe narrow canyons (Figures 2 and 3). In real drainage basins, results provided by the HD coarsening differ from those provided by the NN and CM coarsening especially when complex terrains are considered, with differences that generally increase as the grid cell size h of the coarse digital elevation model increases (Figures 5 and 6, Table 1). This conclusion was supported by the CDF of elevations observed in the considered drainage systems and by the related values of differential entropy (Figure 7 and Table 2). Especially when the attention was focused on grid cells lying along the mainstream, the degradation of information content observed in terms of percentage reduction in differential entropy when high-resolution topographic data are coarsened was found to be significantly smaller when the HD coarsening was used in preference to the NN and CM coarsening (Table 2). In absolute terms, the HD coarsening was found to provide planar descriptions of channels that are affected by acceptable absolute errors (MAPD $< h/2$) and descriptions of channel profiles that are affected by insignificant absolute errors (MAED < 7.92 m), over the whole range of geomorphological settings and grid cell sizes investigated (Figure 9).

The improvements offered by the HD coarsening over the NN and CM coarsening are due to the better ability of the HD coarsening to retain the thalweg profiles of valleys and channels and to reduce the impact of depression-filling in resampled topographic data. The HD coarsening strategy is therefore advocated for all those hydrologic applications where a detailed description of valley and channel thalweg profiles is important and the impact of depression-filling needs to be minimized. The HD coarsening strategy is especially relevant to the description of valleys and channels in landscapes dominated by canyons. In the whole range of geomorphological settings, accurate descriptions of valley and channel profiles are expected to be important to understand and predict surface flow propagation, hyporheic fluxes, and hydrologic interactions between hill slope and channel networks. Future work will be directed to representing the hill slope systems within the coarse grid cells and to describing the dynamic connectivity between channel and hill slope networks in distributed surface-subsurface flow models.

References

Barnes, R., Lehman, C., & Mulla, D. (2014). Priority-flood: An optimal depression-filling and watershed-labeling algorithm for digital elevation models. *Computers & Geosciences*, *62*(1), 117–127. https://doi.org/10.1016/j.cageo.2013.04.024

Bonetti, S., Bragg, A. D., & Porporato, A. (2018). On the theory of drainage area for regular and non-regular points. *Proceedings of the Royal Society of London*, *474*(2211), 20170693. https://doi.org/10.1098/rspa.2017.0693

Bras, R. L. (1990). *Hydrology: An introduction to hydrologic science*. Reading, MA: Addison-Wesley.

Camporese, M., Paniconi, C., Putti, M., & Orlandini, S. (2010). Surface-subsurface flow modeling with path-based runoff routing, boundary condition-based coupling, and assimilation of multisource observation data. *Water Resources Research*, *46*, W02512. https://doi.org/10.1029/2008WR007536

Chen, Y., Wilson, J. P., Zhu, Q., & Zhou, Q. (2012). Comparison of drainage-constrained methods for DEM generalization. *Computers & Geosciences*, *48*(Suppl. C), 41–49. https://doi.org/10.1016/j.cageo.2012.05.002

Cover, T. M., & Thomas, J. A. (2006). *Elements of Information Theory, Wiley Series in Telecommunications and Signal Processing* (748 p.). Hoboken, NJ: Wiley-Interscience.

De Bartolo, S., Dell'accio, F., Frandina, G., Moretti, G., Orlandini, S., & Veltri, M. (2016). Relation between grid, channel, and Peano networks in high-resolution digital elevation models. *Water Resources Research*, *52*, 3527–3546. https://doi.org/10.1002/2015WR018076

Gallant, J. C., & Hutchinson, M. F. (2011). A differential equation for specific catchment area. *Water Resources Research*, *47*, W05535. https://doi.org/10.1029/2009WR008540

Gallant, J. C., & Wilson, J. P. (2000). Primary topographic attributes. In Wilson, J. P. & Gallant, J. C. (Eds.), *Terrain analysis: Principles and applications* (pp. 51–85). New York, NY: John Wiley & Sons.

Grimaldi, S., Nardi, F., Di Benedetto, F., Istanbulluoglu, E., & Bras, R. L. (2007). A physically-based method for removing pits in digital elevation models. *Advances in Water Resources*, *30*(10), 2151–2158.

Hester, E. T., & Doyle, M. W. (2008). In-stream geomorphic structures as drivers of hyporheic exchange. *Water Resources Research*, *44*, W03417. https://doi.org/10.1029/2006WR005810

Hutchinson, M. F. (1989). A new procedure for gridding elevation and stream line data with automatic removal of spurious pits. *Journal of Hydrology*, *106*(1–2), 221–232.

Ivanov, V. Y., Vivoni, E. R., Bras, R. L., & Entekhabi, D. (2004). Catchment hydrologic response with a fully distributed triangulated irregular network model. *Water Resources Research*, *40*, W11102. https://doi.org/10.1029/2004WR003218

Kollet, S. J., & Maxwell, R. M. (2006). Integrated surface groundwater flow modeling: A free-surface overland flow boundary condition in a parallel groundwater flow model. *Advances in Water Resources*, *29*(7), 945–958.

Le Coz, M., Delclaux, F., Genthon, P., & Favreau, G. (2009). Assessment of digital elevation model (DEM) aggregation methods for hydrological modeling: Lake Chad Basin, Africa. *Computers & Geosciences*, *35*(8), 1661–1670. https://doi.org/10.1016/j.cageo.2008.07.009

Leopold, L. B., Wolman, M. G., & Miller, J. P. (1964). *Fluvial processes in geomorphology*. San Francisco, CA: W. H. Freeman.

Martz, L. W., & Garbrecht, J. (1992). Numerical definition of drainage network and subcatchment areas from digital elevation models. *Computers & Geosciences*, *18*(6), 747–761.

McGuire, K. J., & McDonnell, J. J. (2010). Hydrological connectivity of hillslopes and streams: Characteristic time scales and nonlinearities. *Water Resources Research*, *46*, W10543. https://doi.org/10.1029/2010WR009341

Montgomery, D. R., & Foufoula-Georgiou, E. (1993). Channel network source representation using digital elevation models. *Water Resources Research*, *29*(12), 3925–3934.

Moretti, G., & Orlandini, S. (2008). Automatic delineation of drainage basins from contour elevation data using skeleton construction techniques. *Water Resources Research*, *44*, W05403. https://doi.org/10.1029/2007WR006309

O'Donnell, G., Nijssen, G. B., & Lettenmaier, D. P. (1999). A simple algorithm for generating streamflow networks for grid-based, macroscale hydrological models. *Hydrological Processing*, *13*(8), 1269–1275.

Orlandini, S., & Moretti, G. (2009). Determination of surface flow paths from gridded elevation data. *Water Resources Research*, *45*, W03417. https://doi.org/10.1029/2008WR007099

Orlandini, S., Moretti, G., Corticelli, M. A., Santangelo, P. E., Capra, A., Rivola, R., et al. (2012). Evaluation of flow direction methods against field observations of overland flow dispersion. *Water Resources Research*, *48*, W10523. https://doi.org/10.1029/2012WR012067

Orlandini, S., Moretti, G., & Gavioli, A. (2014). Analytical basis for determining slope lines in grid digital elevation models. *Water Resources Research*, *50*, 526–539. https://doi.org/10.1002/2013WR014606

Orlandini, S., Moretti, G., Franchini, M., Aldighieri, B., & Testa, B. (2003). Path-based methods for the determination of nondispersive drainage directions in grid-based digital elevation models. *Water Resources Research*, *39*(6), 1144. https://doi.org/10.1029/2002WR001639

Orlandini, S., & Rosso, R. (1998). Parameterization of stream channel geometry in the distributed modeling of catchment dynamics. *Water Resources Research*, *34*(8), 1971–1985.

Orlandini, S., Tarolli, P., Moretti, G., & Dalla Fontana, G. (2011). On the prediction of channel heads in a complex alpine terrain using gridded elevation data. *Water Resources Research*, *47*, W02538. https://doi.org/10.1029/2010WR009648

Passalacqua, P., Belmont, P., Staley, D. M., Simley, J. D., Arrowsmith, J. R., Bode, C. A., et al. (2015). Analyzing high resolution topography for advancing the understanding of mass and energy transfer through landscapes: A review. *Earth-Science Reviews*, *148*, 174–193. https://doi.org/10.1016/j.earscirev.2015.05.012

Passalacqua, P., Tarolli, P., & Foufoula-Georgiou, E. (2010b). Testing space-scale methodologies for automatic geomorphic feature extraction from lidar in a complex mountainous landscape. *Water Resources Research*, *46*, W11535. https://doi.org/10.1029/2009WR008812

Passalacqua, P., Trung, T. D., Foufoula-Georgiou, E., Sapiro, G., & Dietrich, W. E. (2010a). A geometric framework for channel network extraction from lidar: Nonlinear diffusion and geodesic paths. *Journal of Geophysical Research*, *115*, F01002. https://doi.org/10.1029/2009JF001254

Reed, S. M. (2003). Deriving flow directions for coarse-resolution (1–4 km) gridded hydrologic modeling. *Water Resources Research*, *39*(9), 1238. https://doi.org/10.1029/2003WR001989

Saunders, W. (2000). Preparation of DEMs for use in environmental modelling analysis. In Maidment, D. & Djokic, D. (Eds.), *Hydrologic and hydraulic modelling support with geographic information systems* (pp. 29–51). Redlands, CA: Environmental Systems Research Institute Inc.

Tarolli, P. (2014). High-resolution topography for understanding earth surface processes: Opportunities and challenges. *Geomorphology*, *216*(7), 295–312. https://doi.org/10.1016/j.geomorph.2014.03.008

Wang, M., Hjelmfelt, A. T., & Garbrecht, J. (2000). DEM aggregation for watershed modeling. *Journal of the American Water Resources Association*, *36*(3), 579–584. https://doi.org/10.1111/j.1752-1688.2000.tb04288.x

Wilby, R. L., Hay, L. E., Gutowski, W. J. Jr., Arritt, R. W., Takle, E. S., Pan, Z., et al. (2000). Hydrological responses to dynamically and statistically downscaled climate model output. *Geophysical Research Letters*, *27*, 1199–1202.

Wilson, J. P., & Gallant, J. C. (2000). Digital terrain analysis. In Wilson, J. P. & Gallant, J. C. (Eds.), *Terrain analysis: Principles and applications* (pp. 1–27). New York, NY: John Wiley & Sons.

Zhou, Q., & Chen, Y. (2011). Generalization of DEM for terrain analysis using a compound method. *ISPRS Journal of Photogrammetry and Remote Sensing*, *66*(1), 38–45. https://doi.org/10.1016/j.isprsjprs.2010.08.005